



# OPEN Savanna ecosystems and mammalian adaptations in Mid-Miocene Northern China

Chunxiao Li<sup>1,2</sup>, Shi-Qi Wang<sup>1✉</sup>, Yang Wang<sup>3,4</sup>, Tao Deng<sup>1,2</sup>, Jiao Ma<sup>1</sup>, Bian Wang<sup>1</sup>, Qigao Jiangzuo<sup>1</sup> & Danhui Sun<sup>1</sup>

The paleoenvironments and ecosystems of northern China during the Miocene (ca. 23–5.3 Ma) are complex topics, especially concerning the uplift of the Tibetan Plateau on the surrounding areas and the ecological adaptations of mammals as a consequence. Our data integrated stable carbon and oxygen isotope analysis, cenograms, and hypsodonty of herbivorous mammals. The results reveal open, arid, savanna-like habitats in the Junggar Basin during the late early Miocene (ca. 20.4–15.9 Ma). These habitats subsequently spread to northern China by the late Miocene (ca. 11.6–5.3 Ma), driving mammalian adaptation. Large herbivores, particularly proboscideans and rhinocerotids, exhibited strong adaptations to these new open environments, while smaller taxa maintained a preference for more closed, forested habitats. Additionally, during global climate changes, biodiversity declined, indicating increased ecological pressure. Despite these changes, faunal diets in the Junggar Basin remained consistent. Our findings contribute to understanding mid-Miocene paleoecology in northern China and the adaptive strategies of mammals in response to environmental changes.

**Keywords** Savanna-like habitats, Mammalian adaptation, Northern China, Mid-Miocene, Stable isotope analysis, Open environment

The Late Cenozoic marks a period of significant climatic change on Earth, during which the global climate transitioned from a greenhouse to an icehouse state<sup>1,2</sup>. This shift led to the gradual transformation of mid-latitude forests into grasslands, fostering the development of more open ecosystems<sup>3</sup>. In this context, the evolution and adaptive changes of mammals became a key scientific question. The uplift of the Tibetan Plateau is considered one of the major drivers of Late Cenozoic climate change, affecting global atmospheric circulation, forming the East Asian monsoon, and causing Central Asia's aridification<sup>4–6</sup>. This geological event not only shaped the region's climate but also significantly influenced mammalian evolution<sup>7,8</sup>.

The response of the mammals to the regional climatic change is an interesting question. Especially in the transition of the Mid-Miocene Climatic Optimum (MMCO) and the Mid-Miocene Climatic Transition (MMCT), which is a key period for the Late Cenozoic climatic change. The MMCO (~17–14.5 Ma) was characterized by globally warm and humid conditions, leading to the expansion of forested environments and a diversification of mammalian taxa<sup>9,10</sup>. In contrast, the MMCT (~14.5–13 Ma) marked a shift toward cooler and more arid conditions, driven by declining atmospheric CO<sub>2</sub> levels and Antarctic ice sheet expansion, leading to significant ecological restructuring<sup>1,11</sup>. Previously, the mammalian adaptation to this change has been studied in Europe and North America<sup>12–16</sup>. However, a comprehensive study of its impact on Late Cenozoic faunal changes in Asia, especially backdropped by the elevation of the Tibetan Plateau, is still lacking<sup>17</sup>.

The Junggar Basin and the Tongxin region in China, covering MMCO and MMCT, offer an ideal model for addressing these questions. These regions feature rich fossil records, well-preserved stratigraphy, and reliable paleomagnetic dating<sup>18</sup>. Recent studies on the local changes of vegetation and geochemical records have provided a strong geological and biological basis for studying Late Cenozoic climate change<sup>19,20</sup>. Wang et al.<sup>20</sup> conducted a detailed study on the vegetation of the Junggar Basin, during the MMCT and found that, this region was dominated by xerophytic shrubs and Chenopodiaceae (> 50%), with an increased presence of cold-tolerant coniferous trees such as *Pinus* and *Picea*, indicating a transition to a cooler and more arid climate.

<sup>1</sup>Key Laboratory of Vertebrate Evolution and Human Origins of the Chinese Academy of Sciences, Institute of Vertebrate Paleontology and Paleoanthropology, Chinese Academy of Sciences, Beijing, China. <sup>2</sup>University of Chinese Academy of Sciences, Beijing 100049, China. <sup>3</sup>Department of Earth, Ocean and Atmospheric Science, Florida State University, Tallahassee, FL 32306-4520, USA. <sup>4</sup>National High Magnetic Field Laboratory, Tallahassee, FL 32310, USA. ✉email: wangshiqi@ivpp.ac.cn

The primary aim of this study is to investigate paleoenvironmental changes and mammalian adaptations in northern China and Central Asia during the MMCO and MMCT. To achieve this, we analyze stable carbon and oxygen isotope data from mammals across various faunas, comparing isotope values from China with those from Europe and North America during the same periods. Additionally, we apply tooth hypsodonty and cenogram methods to explore the diversity of herbivorous mammals and examine the differences in feeding strategies and ecological adaptations among different taxa.

## Geological settings

### Geological information of Junggar basin and Tongxin region

The northern Junggar Basin is located in the Xinjiang Uygur Autonomous Regions, at approximately 46.5° latitude and 88.5° longitude, with an elevation of about 500 m. Situated in the non-monsoon zone of Central Asia, this region receives an average annual precipitation of 173.7 mm (Source: <http://data.cma.gov.cn/>). During the Cenozoic era, the continuous subduction of the Indian plate beneath the Eurasian continent led to the intense uplift of the Tibetan Plateau, significantly impacting northern regions. This process resulted in the formation of the Altai Mountains and the subsidence of the Junggar-Hami block, creating continuous sedimentary strata in the Junggar Basin<sup>18,21</sup>.

The Neogene strata in the northern Junggar Basin are well-exposed, with clear stratification and abundant fossils, making the region an ideal site for studying mammalian evolution and climate change. The Cenozoic stratigraphy of the northern Junggar Basin can be divided into six lithostratigraphic units, listed from bottom to top: Ulungur River Formation (Eocene to early Oligocene), Teersihabahe Formation (late Oligocene), Sosoquan Formation (23.3–16.9 Ma), Halamagai Formation (16.9–15.5 Ma), Kekemaideng Formation (15.5–13.1 Ma), and Dingshanyanchi Formation (13.1–6 Ma)<sup>18,22,23</sup>. Each unit has yielded significant mammalian fossils. The Halamagai Formation, characterized by its green color, indicates a reducing sedimentary environment and contains the most abundant mammalian fossils, reflecting a relatively warm and humid environment during the MMCO<sup>21</sup>. In contrast, the Kekemaideng Formation, with its rusty yellow color and lower fossil diversity, suggests a relatively dry and cold environment, possibly corresponding to the MMCT.

The Tongxin, located in the Ningxia Hui Autonomous Regions at approximately 37° latitude and 106° longitude, has an elevation of about 1500 m. This region lies at the margin of the East Asian monsoon, with an average annual precipitation of 478 mm (Source: <http://data.cma.gov.cn/>). The Cenozoic subduction of the Indian plate beneath the Eurasian continent also triggered the Qilian-Liupan orogenesis, contributing to continuous sedimentation in the region<sup>24,25</sup>. The Cenozoic stratigraphy of the Tongxin region is divided into the following units: Sikouzi Formation (Paleocene to Eocene), Qingshuiying Formation (Oligocene to earliest Miocene), Zhanghenbao Formation (18–13 Ma), and Ganhegou Formation (late Miocene)<sup>25</sup>. The Early to Middle Miocene Zhanghenbao Formation consists of five stable cycles of sandstone-mudstone alternations, with abundant mammalian fossils discovered in each layer. According to Wang et al.<sup>19,20</sup>, the lower A–C layers of the Zhanghenbao Formation, dated to approximately 18.0–15.0 Ma, corresponding to the MMCO. The upper D and E layers, date to approximately 14.5–13.3 Ma, coincide with the MMCT.

### Faunas examined and their age and geographic information

In this article, we present a broad comparison of mammalian faunas from mid-latitude regions of Eurasia and North America during the Miocene (Fig. 1). The new data primarily come from the faunas of the Junggar Basin and Tongxin region. Four faunas from these regions were carefully studied:

Northern Junggar Basin:

1. Halamagai (mid-age, 16.2 Ma, MMCO); 2. Kekemaideng (14.3 Ma, MMCT).

Tongxin region:

3. lower Tongxin (16.5 Ma, MMCO); 4. upper Tongxin (13.9 Ma, MMCT).

The members of these faunas (including carnivores, herbivores, and small mammals) are listed in Data 2. The age of these faunas was determined using paleomagnetic dating<sup>18,22</sup>.

For comparison, we also examine the following faunas from previous studies:

1. Tunggur fauna, China, approximately N43.5° E113°, representing age, 12.6 Ma (13.6–11.6 Ma, MMCT)<sup>26</sup>.
2. Tuosu fauna (Qaidam Basin), China, approximately N37° E97°, representing age, 10.7 Ma (11.2–10.2 Ma, Late Miocene)<sup>24</sup>.
3. Lantian Fauna, China, approximately N34° E109.5°, representing age, 9 Ma (10.8–7.2 Ma, Late Miocene)<sup>27</sup>.
4. Baode Fauna, China, approximately N39° E111°, representing age, 6.8 Ma (7.2–6.4 Ma, Late Miocene)<sup>28</sup>.
5. Sandelzhausen (North Alpine foreland basin), Germany, approximately N48.5° E12°, representing age, 16.3 Ma (16.5–16 Ma, MMCO)<sup>13</sup>.
6. Steinheim (North Alpine foreland basin), Germany, N48° E9°, approximately 14.3 Ma<sup>13</sup>.
7. Sansan, France, N43.5° E0.5°, approximately 15 Ma (MMCO/MMCT) (NOW database<sup>29</sup>).
8. Madrid Basin (“lower Madrid”), Spain, including sites such as Somosaguas, Arroyo del Olivar, Barajas 3 and 7, Paseo de las Acacias, Estación Imperial, PAR Peñuelas, San Isidro, Puente de Toledo, La Hidroeléctrica, and Casa de Campo, approximately N40° W4°, representing age, 15.2 Ma (16–14.5 MMCO)<sup>15</sup>.
9. Madrid Basin (“upper Madrid”), Spain, including sites such as Paracuellos 3 and 5, Alhambra-Túneles, Henares 1, and Puente de Vallecas, approximately N40° W4°, representing age, 13.8 Ma (14.5–13 MMCT)<sup>15</sup>.
10. Mascall Formation (“lower Oregon”), Columbia Plateau, Oregon, USA, approximately N44° W118°, representing age, 15.1 Ma (MMCO)<sup>30</sup>.
11. Sucker Creek, Quartz Basin, and Red Basin (“upper Oregon”), Oregon, USA, approximately N44° W118°, representing age, 13.6 Ma (MMCT) (14.8–12.5)<sup>30</sup>.

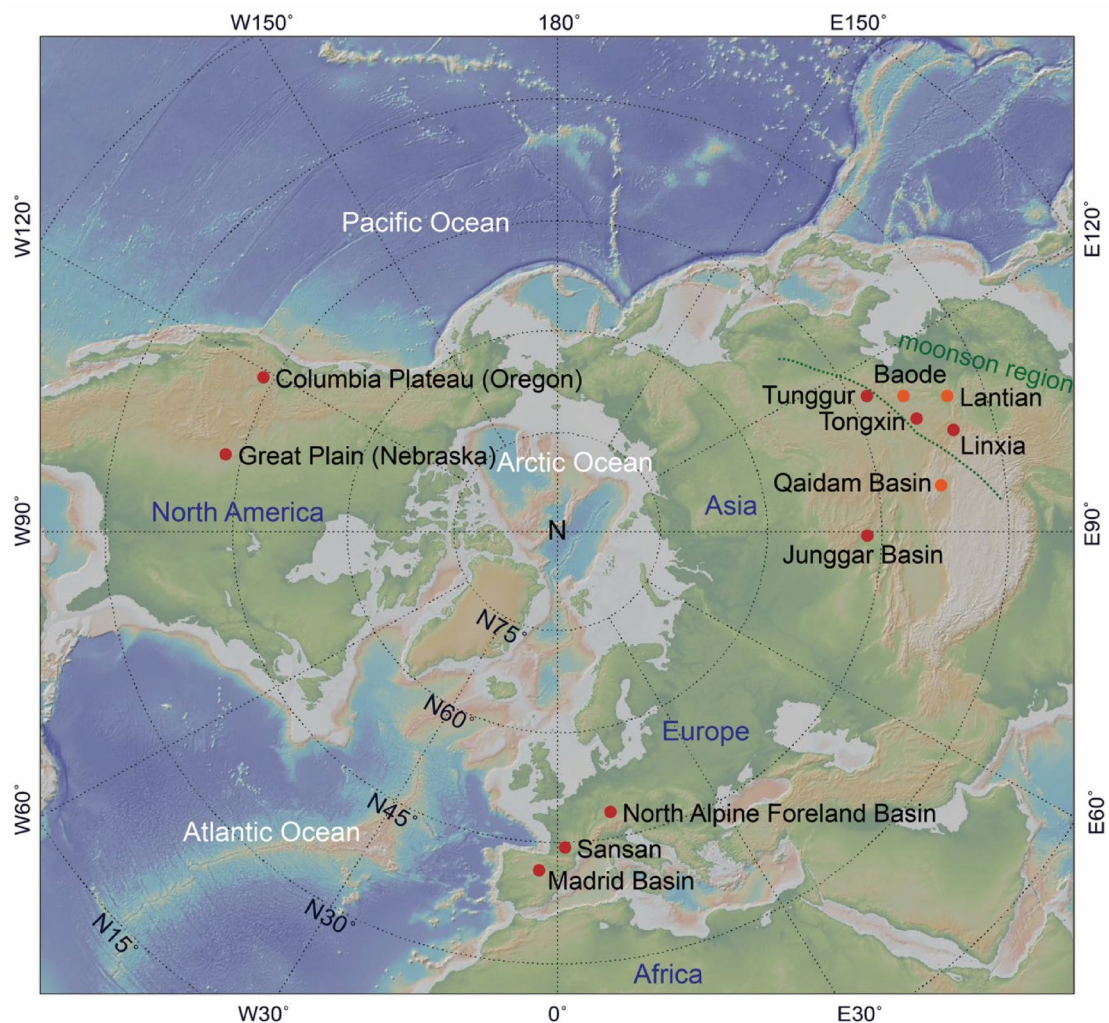


**Fig. 1.** Geographic locations of different fossil sites in the Northern Mid-latitudes. Red circles represent early and middle Miocene study regions, while orange circles indicate late Miocene regions, as mentioned in the text (Table 1). The green dotted line marks the boundary between monsoon/non-monsoon regions. This geographic map was generated using GeoMapApp (V3.6.15) (<https://www.geomapp.org/>).

12. Myers Farm, Valentine Quarry, Norden Bridge, and Hottell Immense, Nebraska, Great Plains, USA, approximately N41° W100°, representing age, 14.2 and 13.1 Ma (MMCT)<sup>31</sup>.

These faunas are all located in the mid-latitude regions of Eurasia and North America, and primarily span the MMCO and MMCT (some extending into the late Miocene). This allows for a comparison of paleoenvironment and mammalian paleoecology in Central and East Asia with those in Europe and North America during major climate transitions in the Neogene. In Table 1, we provide the geographical information for all faunas included in this comparison.

## Methods

### Stable carbon and oxygen isotopes analysis of tooth enamel

We collected 187 enamel samples from fossil teeth of various herbivorous mammals in the Junggar Basin and Tongxin region for stable carbon and oxygen isotope analysis. All tooth specimens from the early and middle Miocene of northern China were housed at the Institute of Vertebrate Paleontology and Paleoanthropology, Chinese Academy of Sciences, Beijing, China. Stable isotope analyses were conducted at the National High Magnetic Field Laboratory, Florida State University, USA.

For comparison, we analyzed previously published  $\delta^{13}\text{C}$  values from other mid-latitude regions (Table 1), including the Linxia Basin and Tunggur region in China, as well as data from Europe and North America, such as Sandelzhausen and Steinheim (Northern Alpine Foreland Basin, Germany), the Madrid Basin (Spain), the Columbia Plateau (Oregon, USA.), and the Great Plains (Nebraska, USA.)<sup>12–15,32–35</sup>. In timeline, we also extend the comparison to late Miocene localities in China, including the Qaidam Basin, Lantian, and Baode regions. For the detailed data sources, please see Data 1.



Latitude range	Region	Fauna	Age interval
Higher than N40°	Atlantic east coast (Europe)	Sandelzhausen	MMCO
		Sansan	MMCO
		Steinheim	MMCT
	Central Asia (non-monsoon)	Halamagai (Junggar Basin)	MMCO
		Kekemaideng (Junggar Basin)	MMCT
	East Asia	Tunggur	MMCT
	Columbia Plateau (North America)	Oregon	MMCO and MMCT
N30°–approximate N40°	Great Plain (North America)	Nebraska	MMCT
	Atlantic east coast (Europe)	Madrid Basin	MMCO and MMCT
	Central Asia (non-monsoon)	Tuosu (Qaidam Basin)	late Miocene
	East Asia (monsoon)	lower Tongxin	MMCO
		upper Tongxin	MMCT
		Linxia Basin	MMCO and MMCT
		Lantian	late Miocene
		Baode	late Miocene

**Table 1.** Geographical information of all faunas compared in this study.

To extract enamel samples, small patches were cut from the tooth or drilled along the entire length using a rotary drill. The samples were ground into fine powder (2–3 mg). These were then pre-treated with 5% sodium hypochlorite (NaOCl) overnight to remove organic contaminants and cleaned with distilled water. The samples were further treated with 1 M acetic acid overnight to remove non-structural carbonates and cleaned again with distilled water. The samples were then freeze-dried<sup>32,36</sup>. The dried enamel samples were reacted with 100% phosphoric acid (H<sub>3</sub>PO<sub>4</sub>) at 25 °C for approximately 72 hours<sup>36,37</sup>.

Carbon and oxygen isotope data were measured using a Finnigan MAT Delta Plus XP stable isotope ratio mass spectrometer coupled with a Thermo Scientific GasBench II at Florida State University. The lab standards used included MERK, MB-CC, ROY-CC, and PDA. Results are reported in the standard delta (δ) notation as δ<sup>13</sup>C<sub>enamel</sub> and δ<sup>18</sup>O<sub>enamel</sub> values relative to the international carbonate standard VPDB (Vienna Pee Dee Belemnite). The diet δ<sup>13</sup>C values of proboscideans using an enrichment factor (ε\*) of 13‰ for non-ruminants like proboscideans, and 14.1‰ for ruminants<sup>36,38</sup>. However, Tejada-Lara et al.<sup>39</sup> demonstrated a strong and significant correlation between δ<sup>13</sup>C enrichment and body mass across herbivorous mammals. For example, ε\*<sub>diet–bioapatite</sub> values vary from 12.89‰ in pigs (*Sus scrofa*) and 14.65‰ in cattle (*Bos taurus*) among Artiodactyla, to 13.2‰ in zebra (*Equus burchelli*) and 14.4‰ in black rhinoceros (*Diceros bicornis*) among Perissodactyla. Smaller-bodied species such as the house mouse (*Mus musculus*) show lower values (9.1‰), with species like the giant panda (*Ailuropoda melanoleuca*), koala (*Phascolarctos cinereus*), and three-toed sloth (Folivora: *Xenarthra*) clustering around 10–10.5‰. According to Tipple et al.<sup>40</sup> estimates, the CO<sub>2</sub> levels in the middle Miocene atmosphere was approximately 2–1.5‰ higher than those of today. When comparing the mean plant δ<sup>13</sup>C values from modern C<sub>3</sub> biomes with those from the middle Miocene in Junggar and Tongxin, several factors were considered: Latitude. C<sub>3</sub> vegetation receiving equivalent light and water has δ<sup>13</sup>C values that vary with latitude by ~0.3‰/10°<sup>41</sup>. Altitude. Carbon isotope values in C<sub>3</sub> vegetation receiving equivalent light and water vary with altitude by ~0.65‰/1000 m<sup>41</sup>.

To assess potential diagenetic alteration, Fourier Transform Infrared Spectroscopy (FTIR) analysis was conducted on a subset of pre-treated samples. The aim was to determine the crystallinity of hydroxyapatite in the enamel, which helps evaluate diagenetic alteration and its impact on the isotopic composition. FTIR analysis was performed using a NICOLET 6700 infrared spectrometer, with the crystallinity of minerals in 20 samples analyzed under the following parameters: resolution of 4 cm<sup>-1</sup>, 32 scans, spectral range of 4000–400 cm<sup>-1</sup>. The analysis revealed that the primary component of the samples is apatite, and for most samples, the Phosphate Crystallinity Index (PCI)—which indicates that higher PCI values correspond to higher mineral crystallinity—fell within the range typical of modern dental enamel apatite (3.5–3.8). The Crystallinity Index (CI) measures the degree of the PO<sub>4</sub><sup>3-</sup> band splitting and is defined by CI = (A<sub>605</sub> + A<sub>565</sub>)/A<sub>590</sub>, where A<sub>x</sub> is the absorbance at wave number x<sup>42,43</sup>. The crystallinity of enamel apatite, along with the carbonate content, showed no significant changes in the samples. Therefore, it can be concluded that most of the mammalian enamel samples have retained their original isotopic information.

To assess regional differences in the carbon enamel isotopic composition of mammals, we conducted two-tailed t-tests on δ<sup>13</sup>C<sub>enamel</sub> values between each pair of regions. Statistical significance was determined at the 95% confidence level (*p* < 0.05). All statistical analyses were performed using PAST software, and the detailed results, including mean differences, t-values, p-values, and significance levels, are provided in the Table 2.

**Cheek tooth hypsodonty**

Analyzing hypsodonty (molar tooth crown height) in large herbivorous mammals from a specific region allows inferences about environmental openness and climatic conditions (e.g., wet or arid conditions) in that

Sample	Mean difference (%)	t	p	Significant difference at 95% CI?
Junggar $\delta^{13}\text{C}$ vs. Tongxin $\delta^{13}\text{C}$	1.07	6.12	5.4591E-09	Yes
Junggar $\delta^{13}\text{C}$ vs. Germany $\delta^{13}\text{C}$	2.17	12.65	7.768E-27	Yes
Junggar $\delta^{13}\text{C}$ vs. Madrid $\delta^{13}\text{C}$	0.55	2.44	0.0164	Yes
Tongxin $\delta^{13}\text{C}$ vs. Germany $\delta^{13}\text{C}$	1.10	7.04	3.8527E-11	Yes
Tongxin $\delta^{13}\text{C}$ vs. Madrid $\delta^{13}\text{C}$	0.52	2.62	0.0098	Yes
Germany $\delta^{13}\text{C}$ vs. Madrid $\delta^{13}\text{C}$	1.61	8.42	6.153E-14	Yes
Junggar $\delta^{13}\text{C}$ vs. Oregon $\delta^{13}\text{C}$	1.58	10.96	4.7565E-24	Yes
Tongxin $\delta^{13}\text{C}$ vs. Oregon $\delta^{13}\text{C}$	0.52	3.72	0.0002	Yes
Germany $\delta^{13}\text{C}$ vs. Oregon $\delta^{13}\text{C}$	0.58	4.25	2.8408E-05	Yes
Madrid $\delta^{13}\text{C}$ vs. Oregon $\delta^{13}\text{C}$	1.03	5.30	2.404E-07	Yes
Nebraska $\delta^{13}\text{C}$ vs. Oregon $\delta^{13}\text{C}$	1.18	10.48	5.5657E-23	Yes
Junggar $\delta^{13}\text{C}$ vs. Nebraska $\delta^{13}\text{C}$	0.40	2.64	0.0088	Yes
Tongxin $\delta^{13}\text{C}$ vs. Nebraska $\delta^{13}\text{C}$	0.67	4.61	6.2455E-06	Yes
Germany $\delta^{13}\text{C}$ vs. Nebraska $\delta^{13}\text{C}$	1.77	12.41	2.3891E-28	Yes
Madrid $\delta^{13}\text{C}$ vs. Nebraska $\delta^{13}\text{C}$	0.15	0.77	0.44	No

**Table 2.** Statistical significance of differences in the mean carbon isotopic compositions of mammals between different regions as determined by two-tailed t-tests.

area<sup>7</sup>. Increased hypsodonty is an adaptive response to the growing need for wear resistance and functional durability. This adaptation arises from the prevalence of fibrous or abrasive vegetation in environments that are progressively more open and arid-adapted<sup>44</sup>. We examined and classified the hypsodonty of herbivorous taxa from several regions, including Halamagai, Kekemaideng, lower Tongxin, upper Tongxin, Tunggur, Tuosu, Lantian, Baode, Sandelzhausen, Steinheim, Sansan, “lower Madrid” and “upper Madrid”, and compared these data with previously published data from North America Great Plain<sup>45</sup>. Our data were primarily sourced from the NOW Database.

Taxa were categorized into three classes: brachyodont (hypsodonty < 0.8), mesodont (between 0.8 and 1.2), and hypsodont (> 1.2). To determine the mean hypsodonty value for each locality, we calculated the average score across its herbivorous species. For genera not found in the database, we measured the crown height (H) and length (L) of the second upper or lower tooth (M2 or m2), and calculated the ratio of H/L (using any typical individual or the population mean. Stacked area graphs of faunal hypsodonty from China, Europe, and North America were plotted across the age sequence. For data sources, please see Data 2.

Cenogram analysis

Cenograms are a useful method for exploring the relationship between the faunal body mass distribution and environmental conditions<sup>46</sup>. We produced cenograms of the following faunas: Halamagai, Kekemaideng, lower Tongxin, upper Tongxin, Tunggur, Tuosu, Lantian, Baode, Sandelzhausen, Steinheim, Sansan, Sangmelina (Cameroon) and Lokori (Kenya). The latter two serve as modern savanna representatives<sup>46</sup>. Cenogram data for Sandelzhausen, Steinheim, and Sansan were taken directly from Costeur et al.<sup>47</sup>. For the remaining faunas, body mass data for each herbivore and small mammal was sourced from previous publications (primarily after NOW database) or estimated using linear regression methods.

For large herbivores, we use the regression equation from Janis<sup>45</sup> as follows:  
 $\log_{10}(\text{mass in kg}) = \text{intercept} + \text{slope} \times \log_{10}(X \text{ in cm})$ ,  
where X represents the m2 or M2 tooth length (using either a typical individual or the mean of a population), and the intercept and slope values were provided by Janis (1990).

For small mammals, we use the regression equation from Legendre<sup>48</sup> as follows:  
 $\ln(\text{mass in g}) = \text{intercept} + \text{slope} \times \ln(X \text{ in mm}^2)$ ,  
where X represents the length  $\times$  width of m1 (using either a typical individual or the mean of a population), and the intercept and slope values were provided by Legendre<sup>48</sup>.

Detailed calculation for each taxon is listed in Data 2 and Data 3. To minimize the influence of different sample sizes across the faunas, we replaced the rank order on the x-axis with the rank percentile.

Results and discussion

$\delta^{13}\text{C}$  and  $\delta^{18}\text{O}$  of tooth enamel of various mammals from Junggar Basin and Tongxin region, northern China

The mean  $\delta^{13}\text{C}_{\text{enamel}}$  value ( $\pm$  standard deviation [SD]) for all Junggar Basin mammals, irrespective of taxon or level, is  $-9.1\text{‰} \pm 1.3\text{‰}$ , ranging from  $-11.5\text{‰}$  to  $-4.9\text{‰}$  for 97 samples ( $n=97$ ) (Fig. 2). Within this fauna, giraffoid with high tooth crowns, possibly belonging to Climacocerotidae (cf. *Vittoria* sp.), has the highest mean  $\delta^{13}\text{C}$  value at  $-6.7\text{‰} \pm 0.2\text{‰}$ , although it is represented by only 2 samples. Proboscidea also have a relatively high mean  $\delta^{13}\text{C}$  value at  $-8.9\text{‰} \pm 1.3\text{‰}$  ( $n=33$ ), as well as the widest range in values, from  $-11.5\text{‰}$  to  $-4.9\text{‰}$ . Among Proboscidea, *Choerolophodon* having the lowest and *Platybelodon* having the highest mean  $\delta^{13}\text{C}$  values. Differences in  $\delta^{13}\text{C}$  values among species likely reflect variations in their habitats and feeding habits. In Junggar Basin, the majority of the fossil mammals exhibited  $\delta^{13}\text{C}$  values consistent with  $\text{C}_3$  feeding, this suggests an

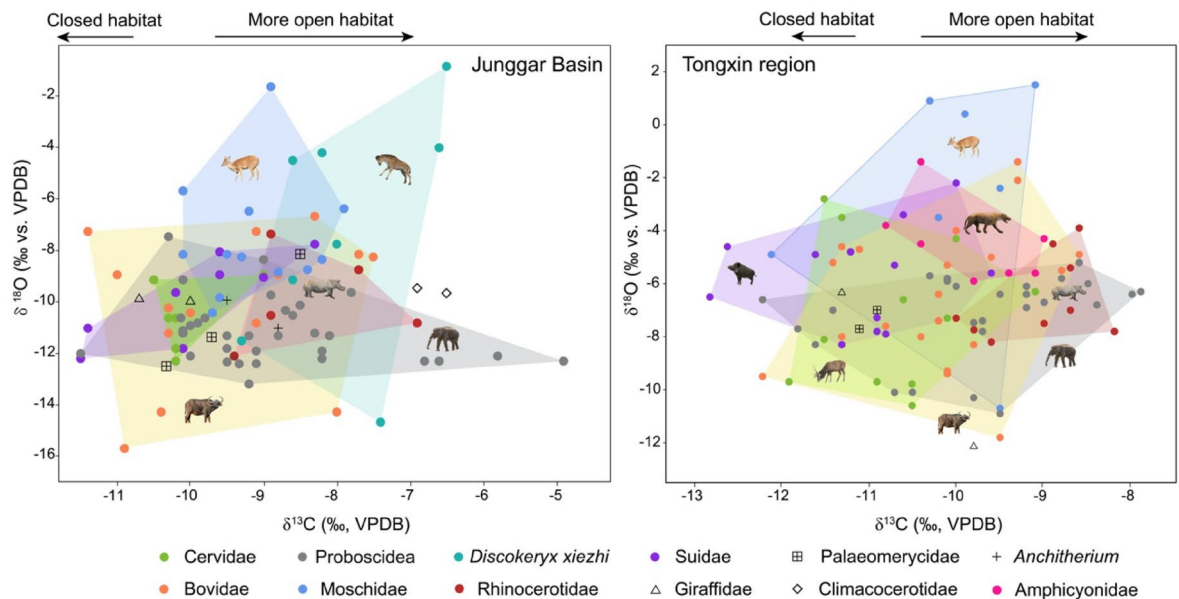


**Fig. 2.** Plot of  $\delta^{13}\text{C}_{\text{enamel}}$  values vs.  $\delta^{18}\text{O}_{\text{enamel}}$  values of various mammals from Junggar Basin and Tongxin Region. Each point represents the  $\delta^{13}\text{C}$  and  $\delta^{18}\text{O}$  values based on bulk samples from one individual tooth.

open habitat primarily dominated by  $\text{C}_3$  plants. Examining proboscidean material in the Junggar Basin, the  $\delta^{13}\text{C}$  values exhibit a notable variation, particularly *Platybelodon* with the highest  $\delta^{13}\text{C}$  values, which suggests variable diets, ranging from a pure  $\text{C}_3$  diet to diets consisting of either mixed  $\text{C}_3$ - $\text{C}_4$  vegetation or primary  $\text{C}_3$  plants under water-stress conditions, and thus an expansion into more open habitats<sup>43</sup>. The taxon displaying the lowest mean  $\delta^{13}\text{C}$  value is Giraffidae, which has a mean  $\delta^{13}\text{C}$  value of  $-10.4\text{‰} \pm 0.3\text{‰}$  ( $n=2$ ). Cervidae have the second lowest mean  $\delta^{13}\text{C}$  value at  $-10.1\text{‰} \pm 0.4\text{‰}$ , ranging from  $-10.5\text{‰}$  to  $-9.3\text{‰}$  ( $n=6$ ). These values suggest that both Giraffidae and Cervidae may have had an affinity for forested habitats and a preference for pure  $\text{C}_3$  diets.

The mean  $\delta^{18}\text{O}_{\text{enamel}}$  value of all Junggar Basin mammals, irrespective of taxon or level, is  $-10.0\text{‰} \pm 2.4\text{‰}$ , with a range from  $-15.8\text{‰}$  to  $-4.2\text{‰}$ . The highest mean  $\delta^{18}\text{O}$  value among the different taxa occurs in the Moschidae, which has a mean value of  $-7.6\text{‰} \pm 2.2\text{‰}$ . This implies that Moschidae primarily sourced their body water from leaf water or significantly evaporated lake/pond water. The proboscidean taxon has the most negative mean  $\delta^{18}\text{O}$  value at  $-11.2\text{‰} \pm 1.2\text{‰}$ , with a range in values from  $-12.4\text{‰}$  to  $-7.5\text{‰}$  ( $n=33$ ), suggesting reliance on relatively stable and less evaporated water sources such as perennial rivers or large lakes. This interpretation is supported by modern isotopic data, which show that surface waters in the Junggar Basin today typically have  $\delta^{18}\text{O}$  values between  $-12\text{‰}$  and  $-6\text{‰}$ <sup>49</sup>. The mean  $\delta^{18}\text{O}$  value of *Discokeryx xiezhi* is  $-7.8\text{‰} \pm 3.6\text{‰}$ , its  $\delta^{18}\text{O}$  values are significantly different from those of all other taxa due to the widest range in values, from  $-14.8\text{‰}$  to  $-4.0\text{‰}$  ( $n=9$ ), exhibiting the greatest overall isotopic variability.

The mean  $\delta^{13}\text{C}_{\text{enamel}}$  value of the Tongxin region mammals was determined to be  $-10.2\text{‰} \pm 1.1\text{‰}$ , closely resembling that of the mammals analyzed from the Junggar Basin (Fig. 2). Notably, Rhinocerotidae displays the highest mean  $\delta^{13}\text{C}$  value of  $-9.1\text{‰} \pm 0.6\text{‰}$ , with values ranging from  $-10.0\text{‰}$  to  $-8.2\text{‰}$  ( $n=9$ ). Suidae, on the other hand, exhibits the most negative mean  $\delta^{13}\text{C}$  value of  $-11.0\text{‰} \pm 0.9\text{‰}$ , with values ranging from  $-12.8\text{‰}$  to  $-9.6\text{‰}$  ( $n=13$ ). Regarding the oxygen isotope data, the mean  $\delta^{18}\text{O}_{\text{enamel}}$  value of all Tongxin Region mammals was determined to be  $-6.4\text{‰} \pm 2.5\text{‰}$ , with a broad range from  $-12.1\text{‰}$  to  $1.5\text{‰}$  ( $n=90$ ). The Moschidae group display the highest mean  $\delta^{18}\text{O}$  value of  $-2.7\text{‰} \pm 4.2\text{‰}$ , with values ranging from  $-10.7\text{‰}$  to  $1.5\text{‰}$  ( $n=7$ ). Palaeomerycidae has the most negative mean  $\delta^{18}\text{O}$  value of  $-7.4\text{‰} \pm 0.4\text{‰}$  ( $n=2$ ). Proboscideans have the second most negative mean  $\delta^{18}\text{O}$  value of  $-7.2\text{‰} \pm 1.5\text{‰}$ , encompassing a range from  $-10.3\text{‰}$  to  $-5.2\text{‰}$  ( $n=26$ ).

The isotopic differences among species may indicate resource partitioning. Previous studies have shown that the  $\delta^{18}\text{O}$  of enamel in obligate drinkers generally reflect the  $\delta^{18}\text{O}$  of local water sources<sup>50,51</sup> whereas non-obligate drinkers are more strongly influenced by the  $\delta^{18}\text{O}$  of food plants. Besides, in the Junggar Basin, the low  $\delta^{18}\text{O}_{\text{enamel}}$  values likely reflect consumption of cold, high-altitude waters with limited seasonal variation, due to low summer rainfall and minimal evaporation. In contrast, higher  $\delta^{18}\text{O}_{\text{enamel}}$  values observed in Tongxin specimens suggest a mixed water sources and strong seasonality. During the summer, monsoonal rainfall and evaporation likely enriched surface water  $\delta^{18}\text{O}$ . For a paleoenvironmental perspective, the  $\delta^{18}\text{O}$  contrast implies that the Miocene climate of Junggar Basin was characterized by a cooler, more continental and non-monsoonal regime with less evaporative moisture loss. In comparison, Tongxin region likely experienced warmer, more seasonal conditions, influenced by summer monsoon incursions and greater aridity.

### Stable isotopes in tooth enamel from different regions during the miocene

Figure 3 clearly show that the  $\delta^{13}\text{C}_{\text{enamel}}$  values from the Junggar Basin are generally less negative compared to those from other regions, particularly during the MMCO, a globally warm and humid period. The  $\delta^{13}\text{C}$  values from the Halamagai in the Junggar Basin are significantly higher than those from Tongxin and Linxia (monsoon margin), suggesting a more arid environment. The higher  $\delta^{13}\text{C}$  values in enamel from the Junggar Basin indicate either severe water-stressed conditions or the consumption of small amounts of  $\text{C}_4$  grasses by some animals<sup>32</sup>. Wang et al.<sup>19</sup> identified  $\text{C}_4$  components in both pollen and paleosols from the strata of Halamagai, indicating that some mammals may have partially consumed  $\text{C}_4$  plants, although  $\text{C}_4$  plants were not a major part of their diet. The  $\delta^{13}\text{C}_{\text{enamel}}$  values of the Kekemaideng fauna are also relatively high, approaching those of Halamagai, and being less negative than those of the Tongxin and Linxia in the monsoon region, as well as the Tunggur fauna in the marginal monsoon region. Notably, only the  $\delta^{13}\text{C}$  range from Nebraska, in the Great Plains of the USA, approaches that of the Kekemaideng fauna (Fig. 3; Table 2). Nevertheless, the  $\delta^{13}\text{C}$  values from the Junggar Basin suggest the most open ecological environment and driest climate conditions across the mid-latitudes of the Northern Hemisphere. Kaya et al.<sup>52</sup> based on the genus-level faunal resemblance index and paleoclimate modeling, proposed that the Baode fauna belongs to the Old World savanna palaeobiome of Central Asia. In

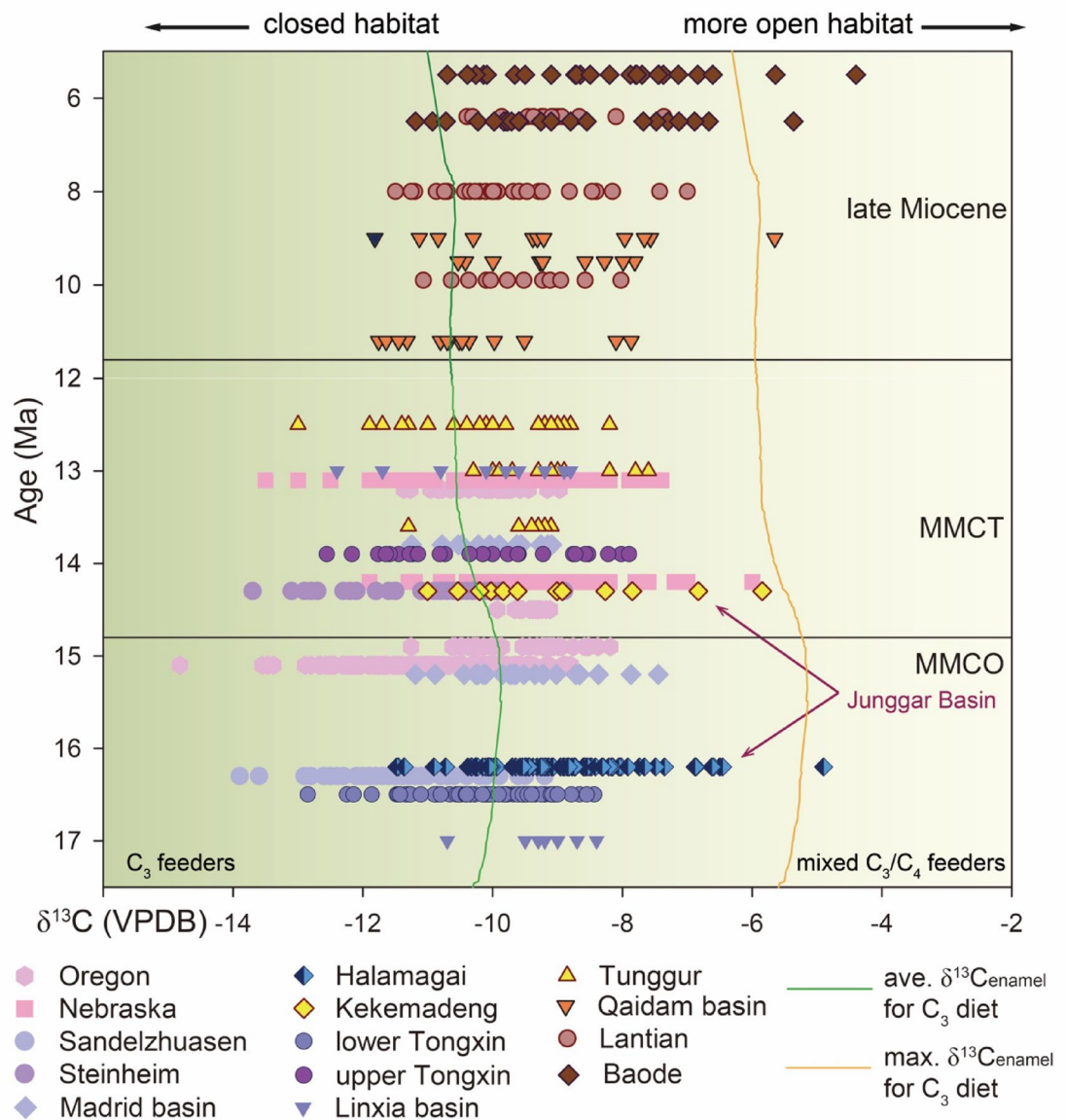


**Fig. 3.** Plot of  $\delta^{13}\text{C}_{\text{enamel}}$  values of various mammals across different regions from 18–5 Ma. The green and yellow curves represent the average and maximum enamel  $\delta^{13}\text{C}$  values for  $\text{C}_3$  diet, respectively, adjusted for past changes in the  $\delta^{13}\text{C}$  of atmospheric  $\text{CO}_2$  (Tippie et al., 2010). Data source: Sandelzhausen (Tütken et al. 2009); Steinheim (Tütken et al., 2006); Madrid Basin (Domingo et al., 2012); Oregon (Drewicz, 2018); Nebraska (Nguy and Secord, 2022); Linxia Basin (Wang and Deng, 2005); Qaidam Basin (Zhang et al., 2012); Tunggur region (Zhang et al., 2009); Baode and Lantian regions (Passey et al., 2009); others, this study.



the Junggar Basin, there were noticeably higher  $\delta^{13}\text{C}$  values during the Mid-Miocene, ranging from  $-11.5\text{‰}$  to  $-6.5\text{‰}$ , with an average of  $-9.1 \pm 1.3\text{‰}$ . This range is closely similar to that of the Baodean fauna ( $-11.5\text{‰}$  to  $-4.4\text{‰}$ , average  $-8.6 \pm 1.5\text{‰}$ ), reflecting a relatively open or arid paleo-environment in Junggar Basin, similar to open and savanna habitats in the Baode region. The fauna of the Junggar Basin points to an open savanna-like environment.

The Junggar Basin ( $46^{\circ}$ – $47^{\circ}\text{N}$ ) and the North Alpine Foreland Basin ( $48^{\circ}$ – $49^{\circ}\text{N}$ ) have similar latitudes, but they diverge in terms of aridity and openness, clearly revealed by the tooth enamel  $\delta^{13}\text{C}$  data (Fig. 3; Table 2). While the North Alpine Foreland Basin was relatively humid during the Miocene, benefiting from moisture brought by westerlies from the Atlantic, the Junggar Basin, and more broadly the Central Asian region, experienced a markedly arid climate<sup>53</sup>. This aridity is thought to have been driven by several factors during the Miocene. First, the uplift of the Tibetan Plateau has contributed to the arid conditions during the late Cenozoic<sup>54,55</sup>. Second, the retreat of the Paratethys Sea has led to reduced rainfall, further intensifying aridity<sup>56</sup>. Last, global cooling has resulted in reduced water vapor and increased drought in Central Asia<sup>57</sup>. In contrast to the North Alpine Foreland Basin, where westerly moisture from the Atlantic provides humidity, the moisture reaching the Junggar Basin from the west is significantly depleted. Only the Indian Ocean monsoon contributes some summer precipitation to the region. Because of these influences, the Junggar Basin remains relatively arid overall.

The MMCO and MMCT represent key climatic events during the Middle Miocene. Around 14 million years ago (Ma), global temperatures began to decline, coinciding with the expansion of the Antarctic ice sheet, marking the onset of the MMCT<sup>58</sup>. In China, several indicators, such as pollen records, chemical weathering patterns, and anisotropy of magnetic susceptibility (AMS), demonstrate changes between the MMCO and MMCT<sup>19,57</sup>. However, tooth enamel stable carbon and oxygen isotope data from different regions do not show significant changes around the MMCT, which may suggest that despite environmental transformations, faunal dietary preferences in mid-latitude Eurasia remained largely unchanged. This implies that these mammals did not rapidly adjust their diets in response to the evolving climate. Both the northern Junggar Basin and the Tongxin region experienced a marked decline in biodiversity (Fig. 4), indicating heightened competition and ecological pressures driven by deteriorating climatic conditions. These pressures likely forced species to either adapt, migrate, or face extinction (see below).

### Herbivorous feeding ecology changes during the miocene

The feeding ecology of large herbivores (e.g., proportion of browsers, mixed feeders, and grazers) can reflect local paleoenvironment conditions. In the present analysis, we counted the numbers of brachydont, mesodont, and hypsodont taxa and their proportions within relevant faunas to roughly access their feeding ecology, following the method of Janis<sup>45</sup>. In Fig. 4, European faunas show very high ratios of brachydont taxa, with mesodonts and hypsodonts being very rare in both in MMCO and MMCT. Europe remained wet and maintained closed habitats during the MMCT, resulting in minimal changes in herbivore feeding ecology despite the global cooling event. In Central and East Asia and North America, the proportions of the three categories are similar, with high proportions of brachydont and mesodont taxa, and few hypsodont taxa. Interestingly, during the MMCT in Central and East Asia, the total number of herbivores decreased greatly, with a considerable loss of brachydonts and mesodonts. In contrast, North America showed an obvious increase in brachydonts and overall herbivores during the MMCT, even though both Asia and America displayed open woodland and savanna-like ecosystems. This suggests that the global cooling of the MMCT had an impact on mammal diversity in Central and East Asia, possibly because these faunas were located in non-monsoon or monsoon margin regions, which are more sensitive to global climatic changes. Given that the  $\delta^{13}\text{C}_{\text{enamel}}$  and  $\delta^{18}\text{O}_{\text{enamel}}$  show little differences between MMCO and MMCT in Halamagai and Tongxin faunas, it could be inferred that large herbivores continued to utilized similar plant sources, although the global cooling event may have led to a decline in plant. This, in turn, likely intensified interspecific competition and caused a loss in large herbivore diversity. The Tuosu fauna of Qaidam Basin at 11–10 Ma shows the lowest ratio of brachydonts and highest ratio of hypsodonts, indicating dry conditions in the non-monsoon region of Central Asia (Fig. 4), possibly due to the high elevation of northern Tibetan Plateau during this period<sup>54</sup>. In the Tuosu fauna, the genera present are entirely new to Central and East Asia (either migrated from elsewhere, like *Hipparion*, or newly evolved, see Data 2). However, in the Late Miocene of East Asia, compared with the faunas of the Great Plains of North America, the numbers of brachydonts and mesodonts are relatively high, potentially due to the relatively wetter conditions caused by the intensification of East Asian monsoon system<sup>19,20</sup>.

### Mammalian adaptation to open environments

To examine the adaptation of various mammals to open environments, we compared  $\delta^{13}\text{C}_{\text{enamel}}$  values across different mammalian groups from Junggar Basin, Tongxin region, Germany, Spain, and the USA during the MMCO and MMCT (Fig. 5). The groups analyzed include elephantiforms, rhinos, horses, large and small size ruminants, and camelids. Each group likely occupied similar ecological niches within their respective fossil communities. Biome classification follows Nguy and Scoed<sup>31</sup>.

Elephantiformes (non-deinotheres proboscideans) (Fig. 5a): Proboscideans in the Junggar Basin exhibit the highest  $\delta^{13}\text{C}$  ranges across all regions, even compared with any other mammalian groups in any regions. As the largest members of these communities, proboscideans showed a strong tendency to expand into open environments, particularly in the Junggar Basin and Tongxin region, where *Platybelodon* played a significant role in this expansion<sup>23</sup>. *Platybelodon*, adapt at consuming grass in open habitats, utilizing its well-developed trunks to gather grasses and then its shovel-shaped lower jaws to cut them<sup>23</sup>. In Europe and North America, proboscideans were mainly represented by *Gomphotherium*<sup>59</sup> which lived in relatively closed environments (e.g., woodland or grassland margins) than *Platybelodon*.



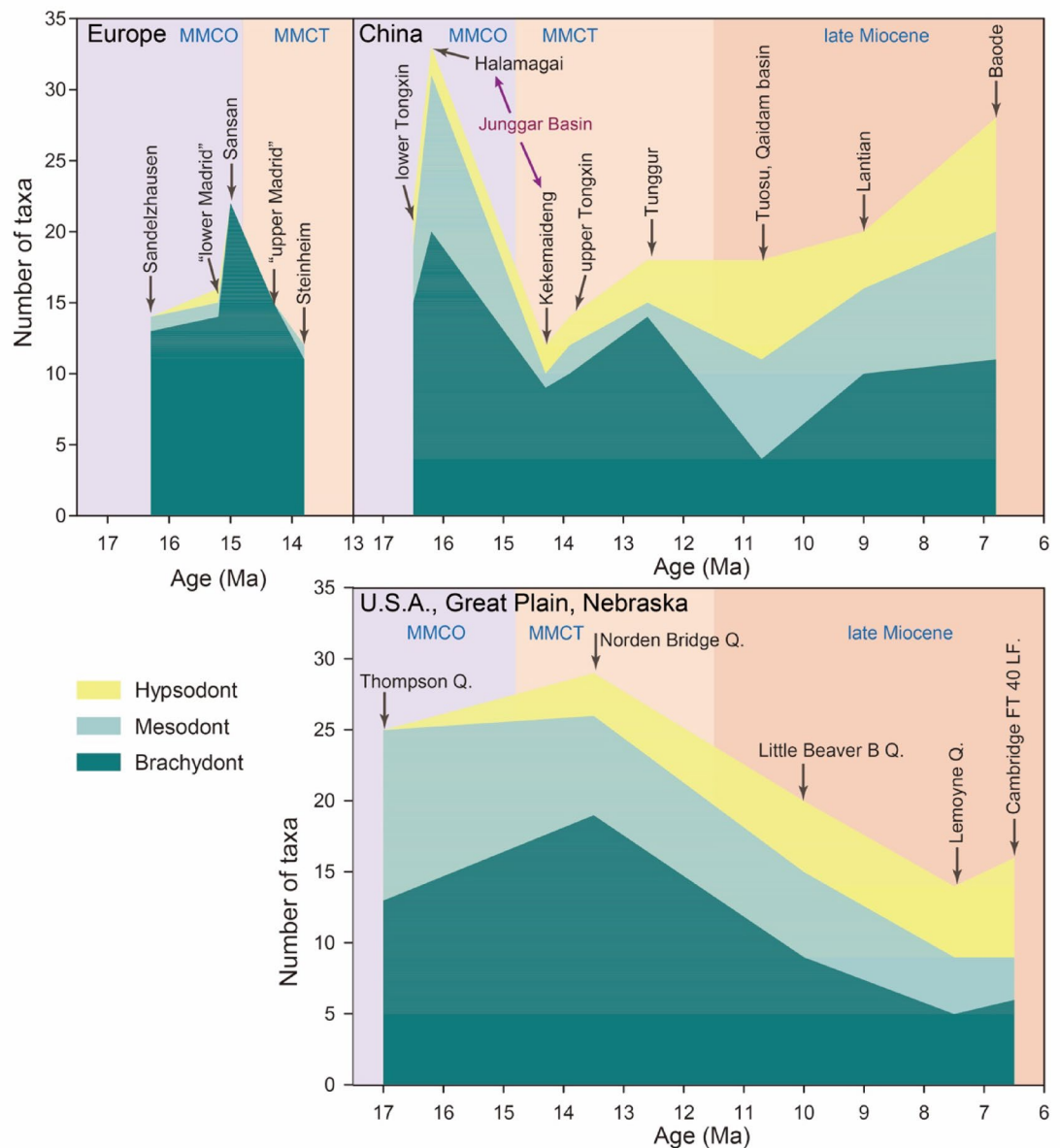


**Fig. 4.** Stacked area plots representing the diversity of large herbivores in representative mid-latitude faunas, categorized into three groups: hypsodonts (yellow), mesodonts (light cyan), and brachydonts (dark green). Data for the U.S.A. are from Janis (2000).

Rhinocerotidae (Fig. 5b): As the second largest mammalian group after proboscideans, rhinoceroses displayed  $\delta^{13}\text{C}$  patterns similar to those of proboscideans during the MMCO period, with the highest mean  $\delta^{13}\text{C}$  values observed in Junggar Basin and the lowest in Germany. Rhinocerotids also showed a clear tendency for expansion into open environments across all regions, except in Germany. In China and Spain, elasmotheriines (*Hispanotherium*, *Tongxinotherium* and *Caementodon*) were prominent components<sup>60</sup>. These taxa developed high-crowned cheek teeth with substantial cementum, which allowed them to feed on grasses in more open habitats. In contrast, German rhinos were primarily represented by the low-crowned species *Brachypotherium* and *Lartetotherium*<sup>61</sup> which likely inhabited relatively closed environments or riparian zones within more open landscapes<sup>31</sup>. In North America, the typical rhino was *Teleoceras*, a hippo-like amphibious mammal<sup>62</sup> which also exhibited adaptations for expansion into more open environments.

Equidae (Fig. 5c): Horses exhibited significant diversity in North America, encompassing both low-crowned Anchitheriinae and high-crowned Equinae (*Hipparioni* and *Equini*). These groups occupied a wide range of ecological niches<sup>63</sup>. The equines, in particular, demonstrated strong adaptations to open environments<sup>31</sup>. Notably,  $\delta^{13}\text{C}$  values from North American horses show an increasing shift between MMCO and MMCT, indicating a significant adaptive transition. The rapid evolution and spread of high-crowned Equinae during MMCT likely facilitated their adaptation to the increasingly open habitats, setting the stage for their eventual migration into

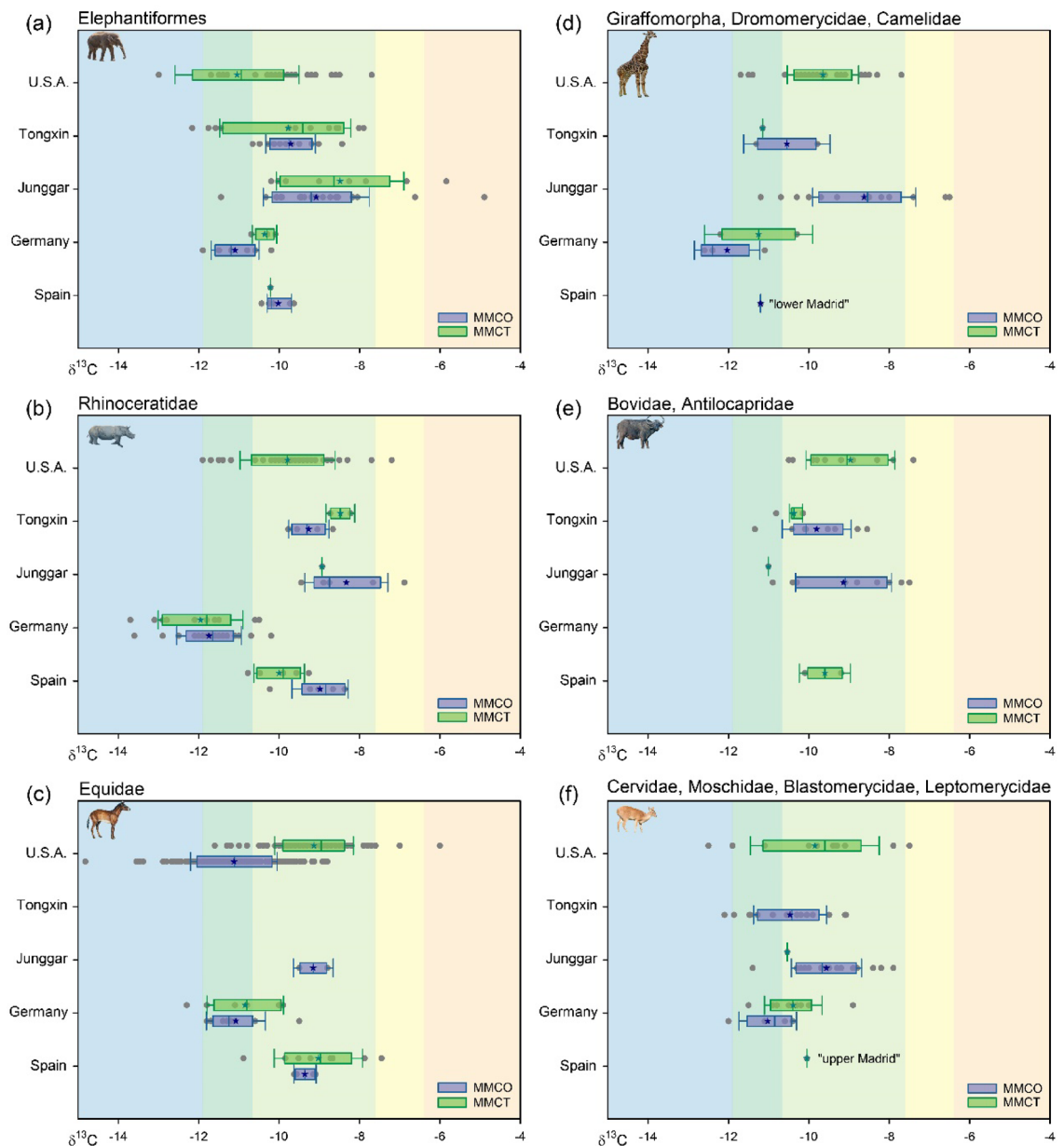


**Fig. 5.**  $\delta^{13}\text{C}_{\text{enamel}}$  values of various herbivorous mammals from MMCO and MMCT localities across Junggar Basin, Tongxin region, North Alpine foreland Basin (Germany), Madrid Basin (Spain), Oregon and Nebraska (U.S.A.), illustrating the adaptation of different taxa to open environments. (a) Elephantiformes (non-deinother proboscideans), (b) Rhinocerotidae, (c) Equidae, (d) Giraffomorpha (Giraffidae, Prolibytheriidae, Climacoceratidae, and Palaeomerycidae), Dromomerycidae, and Camelidae (tall ruminants and camelids), (e) Bovidae and Antilocapridae (high-crowned ruminants), (f) Cervidae, Moschidae, Blastomerycidae, and Leptomerycidae (low-crowned ruminants). The color spectrum in each panel represents different biomes (Nguy and Secord, 2022): blue, closed canopy; dark green, possible riparian within open canopy; light green, open canopy; yellow, water-stressed  $\text{C}_3$  biomes; orange, mixed  $\text{C}_3/\text{C}_4$  biomes. Gray circles represent individual sample points, the stars represent means  $\delta^{13}\text{C}$  values, error bars show the standard deviation, and boxes represent the medians and quartiles for each group.

Eurasia in the late middle Miocene. In Eurasia, *Anchitherium* was the only equids genus<sup>64</sup>. Despite their low-crowned teeth, *Anchitherium* also exhibited adaptations to more open habitats, particularly in Junggar and Spain.

Tall ruminants and Camelidae (Fig. 5d): In large ruminants, Giraffoids were confined in Eurasia, while dromomerycids were found in North America. Although camelids of North America are not ruminants, their similar body type suggests that they likely occupied niches comparable to those of giraffoids<sup>65</sup>. The giraffoids in the Junggar Basin showed a strong adaptation to open environments, particularly the high-crowned taxa such as *Discokeryx xiezhi*<sup>22</sup> and *Vittoria* sp. In contrast, in other Eurasia regions, low-crowned palaeomerycids inhabited

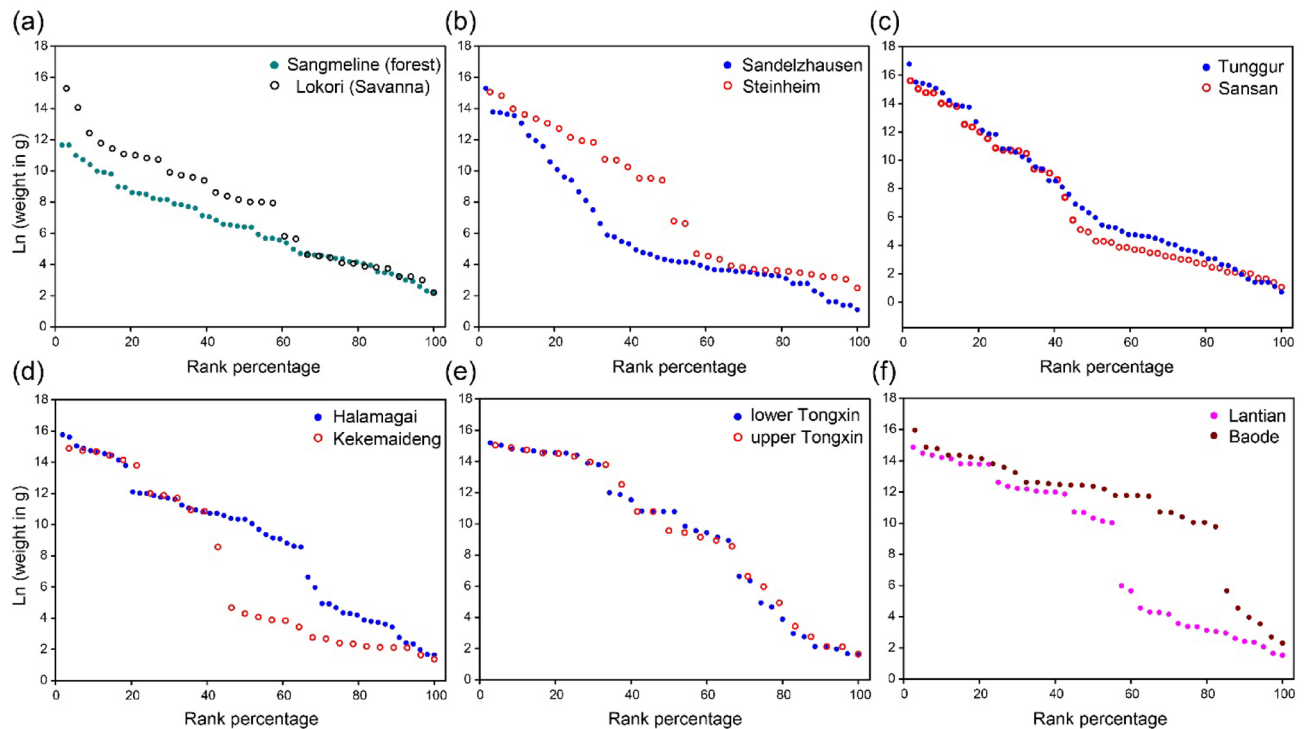


**Fig. 6.** Cenograms of mammalian assemblages from different regions. (a) modern faunas: Sagemelina, Cameroon (forest), and Lokori, Kenya (savanna) (data from Legendre 1989), (b) Junggar Basin, (c) Tongxin region, (d) Sansan (data from Costeur et al., 2012) and Tunggur, (e) North Alpine foreland Basin (data from Costeur et al., 2012), (f) Lantian and Baode. The blue solid and red open circles represent MMCO and MMCT mammalian assemblage, respectively.

relatively closed environments. Camelids from North America also indicate adaptations to open environments, though their adaptations were not as pronounced as those of giraffoids in the Junggar Basin.

Small-sized ruminants (Fig. 5e, f): Bovids (in Eurasia) and antilocaprids (in North America) are small-sized, high-crowned ruminants<sup>66</sup>. Across all regions, they exhibited stronger adaptations to open environments compared to the small, low-crowned ruminants (such as cervids and moschids in Eurasia, and blastomerycids and leptomerycids [*Pseudoparablastomeryx*] in North America)<sup>67</sup> although the differences are not large. Interestingly, despite having higher tooth crowns, the  $\delta^{13}\text{C}$  values of bovids were lower than those of the giraffoids in the Junggar Basin. This suggests that body size may have been a more significant factor in determining the ability to expand into open environments. As bovids generally increased in size during the late Miocene, they demonstrated an enhanced ability to occupy more open habitats.

Environmental changes during the Miocene likely influenced mammalian evolution, with different animals exhibiting varying abilities to expand into open environments in China. Large mammals, such as Rhinocerotidae and Proboscidea, showed a greater tendency to spread into more open environments. In contrast, medium-sized to small mammals, such as cervids, tended to prefer riparian areas within woodlands or relatively closed forests. This difference in habitat preference suggests that factors beyond just environmental changes played a role in shaping mammalian distribution. Among these, size and body mass appear to be one of the primary factors influencing the ability to expand into more open environments.

### Cenograms reveal a savanna environment since the late early miocene of central Asia

The cenogram is an effective method for estimating the structure of the mammalian community, especially for distinguishing between closed and open environments (Fig. 6a). It was observed that Sandelzhausen and Sansan (MMCO) had more medium-sized mammals and a smaller break, which may indicate a more closed environment than that of China (Fig. 6b, c). This is consistent with stable carbon and oxygen isotope data, which reflect a relatively closed environment and humid climate in Europe. In contrast, a break appears in the cenogram of Steinheim fauna, indicating the emergence of a relatively open habitat in the North Alpine Foreland Basin during MMCT.

In Central and East Asia, the records of the Halamagai and upper Tongxin faunas (MMCO) are relatively complete (Fig. 6d, e), revealing a noticeable gap in the cenogram. This gap occurs between  $\ln 6.6$ – $\ln 9$  (body mass between 0.76 kg and 10 kg) (Data 3), indicating the absence of medium-sized herbivores and cenograms suggest open environment. This pattern of weight distribution is similar to that of a modern savanna climate but with a higher prevalence of extremely large animals (greater than  $\ln 12$  or 178 kg). This suggests a climate potentially moister than the contemporary savanna, which could support more megafauna. The number between  $\ln 16$ – $\ln 14$  in the Kekemaideng and upper Tongxin faunas was greater than in modern Lokori.

The mammalian diversity of the Kekemaideng and upper Tongxin faunas (MMCT) is significantly reduced. Although the fossil records are incomplete, the gap of medium-sized herbivores remains present (Fig. 6d, e), indicating an open environmental structure. In contrast, the cenogram of Tunggur region (MMCT, monsoon margin) become more continuous, possibly associated with increased ecological abundance due to the strengthened East Asian monsoon (Fig. 6c). By the late middle Miocene, in Lantian and Bode faunas, the gap in medium-sized herbivores further increased, reflecting a more intensified open environment (Fig. 6f). Estimating body mass and distinguishing foregut from hindgut digesters can enable more refined paleoecological reconstructions<sup>68</sup> particularly by applying different isotopic enrichment factors to better estimate the proportion of C<sub>4</sub> and C<sub>3</sub> plants in paleodiets<sup>68</sup>. In future studies, we plan to incorporate body mass and digestive physiology into our analyses to improve the accuracy of paleoecological reconstructions. Collectively, these results indicate that open savanna-like environments appeared in northern China and Central Asia as early as the late early Miocene.

## Conclusions

This study, through a comprehensive comparison of stable carbon and oxygen isotope data, cenogram analysis, and hypsodonty, reveals the evolution of open habitats and the adaptive strategies of mammals in northern China and Central Asia during the Miocene.

By comparing isotope data across different regions, we observed relatively high  $\delta^{13}\text{C}$  values in the Junggar Basin, indicating either a more open habitat or water-stressed conditions. Cenogram analysis, along with tooth hypsodonty, also supports the emergence of open and savanna habitats in northern China as early as the late early Miocene. This pattern became more pronounced in the Kekemaideng, Lantian, and Baode faunas of the middle to late Miocene, indicating that open savanna-like habitats widespread in northern China and Central Asia from the middle Miocene to late Miocene.

In terms of mammalian adaptation to open environments, large herbivores such as proboscideans, rhinocerotids, and giraffoids were the first to expand into open landscapes. *Platybelodon* played a key role in this transition in the Junggar Basin and Tongxin region, demonstrating a high degree of adaptation to open, savanna-like habitats. Meanwhile, bovids and antilocaprids showed potential for adaptation to open environments, but their expansion was less pronounced compared to larger taxa. In North America, equids exhibited a significant ecological shift, particularly during the MMCT, as high-crowned Equinae rapidly diversified in response to increasingly open habitats. In contrast, small-sized ruminants tended to prefer riparian areas within woodlands or relatively closed forests. Despite significant environmental changes,  $\delta^{13}\text{C}_{\text{enamel}}$  and  $\delta^{18}\text{O}_{\text{enamel}}$  data suggest that mammalian dietary preferences remained relatively stable across the MMCT, with many species continuing to rely on their original plant resources. This likely intensified interspecific competition, ultimately leading to a decline in species diversity. This trend ended in the early late Miocene, when high-crowned taxa became dominant, marking a further stage of mammalian adaptation to open environments.

In conclusion, our findings suggest that open savanna habitats emerged in northern China as early as the late early Miocene and expanded further during the late Miocene. Mammalian adaptation to these changes exhibited a size-dependent pattern, with large-bodied taxa leading the initial expansion, followed by high-crowned taxa, which became dominant in the late Miocene. This ecological transition not only highlights parallel evolutionary trends between East Asia and North America during the Miocene but also provides key paleoecological insights into the formation of modern grassland ecosystems.

## Data availability

Data is provided within the manuscript or supplementary information files.

Received: 7 March 2025; Accepted: 4 July 2025

Published online: 15 July 2025

## References

1. Zachos, J., Pagani, M., Sloan, L., Thomas, E. & Billups, K. Trends, rhythms, and aberrations in global climate 65 ma to present. *Science* **292**, 686–693 (2001).
2. LaRiviere, J. P. et al. Late miocene decoupling of oceanic warmth and atmospheric carbon dioxide forcing. *Nature* **486**, 97–100 (2012).
3. Strömberg, C. A. E. Evolution of grasses and grassland ecosystems. *Annu. Rev. Earth Planet. Sci.* **39**, 517–544 (2011).
4. An, Z., Kutzbach, J. E., Prell, W. L. & Porter, S. C. Evolution of Asian monsoons and phased uplift of the Himalaya–Tibetan plateau since late miocene times. *Nature* **411**, 62–66 (2001).
5. Dupont-Nivet, G. et al. Tibetan plateau aridification linked to global cooling at the Eocene–Oligocene transition. *Nature* **445**, 635–638 (2008).
6. Clift, P. D. et al. Correlation of Himalayan exhumation rates and Asian monsoon intensity. *Nat. Geosci.* **1**, 875–880 (2008).
7. Fortelius, M. et al. Fossil mammals resolve regional patterns of Eurasian climate change during 20 million years. *Evol. Ecol. Res.* **4**, 1005–1016 (2002).
8. Deng, T. et al. Evolution of the Chinese neogene mammalian faunas and its relationship to uplift of the Tibetan plateau. *Adv. Earth Sci.* **30**, 407 (2015).
9. Tian, J., Yang, M., Lyle, M. W., Wilkens, R. & Shackford, J. K. Obliquity and long eccentricity pacing of the middle miocene climate transition. *Geochem. Geophys. Geosyst.* **14**, 1740–1755 (2013).
10. Steinthorsdottir, M. et al. The miocene: the future of the past. *Paleoceanogr Paleoclimatol.* **36**, e2020PA004037 (2021).
11. Frigola, A., Prange, M. & Schulz, M. Boundary conditions for the middle miocene climate transition (MMCT v1.0). *Geosci. Model. Dev.* **11**, 1607–1626 (2018).
12. Tütken, T., Vennemann, T. W., Janz, H. & Heizmann, E. P. J. Palaeoenvironment and palaeoclimate of the middle miocene lake in the Steinheim basin, SW germany: A reconstruction from C, O, and Sr isotopes of fossil remains. *Paleoceanogr Paleoclimatol.* **241**, 457–491 (2006).



13. Tütken, T. & Vennemann, T. W. Stable isotope ecology of miocene large mammals from sandelzhausen, Southern Germany. *Paläontol. Z.* **83**, 207–226 (2009).
14. Martin, C., Bentaleb, I. & Antoine, P. O. Pakistan mammal tooth stable isotopes show paleoclimatic and paleoenvironmental changes since the early oligocene. *Palaeogeogr. Palaeoclimatol. Palaeoecol.* **311**, 19–29 (2011).
15. Domingo, L. et al. Isotopic paleoecology of mammals and the middle miocene cooling event in the Madrid basin (Spain). *Palaeogeogr. Palaeoclimatol. Palaeoecol.* **339**, 98–113 (2012).
16. Aiglstorfer, M., Bocherens, H. & Böhme, M. Large mammal ecology in the late middle miocene Gratkorn locality (Austria). *Palaeobiodiversity Palaeoenviron.* **94**, 189–213 (2014).
17. He, J. K. et al. Evolutionary history of zoogeographical regions surrounding the Tibetan plateau. *Commun. Biol.* **3**, 415 (2020).
18. Ye, J. et al. The Duolebulejin section of Northern Junggar basin and its stratigraphic and environmental implication. *Sci. China Earth Sci.* **42**, 1523–1532 (2012).
19. Wang, J. et al. C4 expansion of central Asia in the middle miocene linked to the strengthening Indian monsoon. *Glob. Planet. Change.* **224**, 104096 (2023).
20. Wang, J. et al. Steppe development and mammalian adaptation in the middle miocene, North Junggar basin, central Asia. *Palaeogeogr. Palaeoclimatol. Palaeoecol.* **659**, 112634 (2024).
21. Meng, J. et al. The neogene Dingshanyan formation in Northern Junggar basin of Xinjiang and its stratigraphic implications. *Vert. Palaeoasiat.* **46**, 90–110 (2008).
22. Wang, S. Q. et al. Sexual selection promotes giraffoid head-neck evolution and ecological adaptation. *Science* **376**, ab18316 (2022).
23. Li, C. X., Deng, T. & Wang, Y. The trunk replaces the longer mandible as the main feeding organ in elephant evolution. *eLife* **12**, RP90908 (2024).
24. Wang, X. M. et al. Early explorations of Qaidam basin (Tibetan Plateau) by birger Bohlin—reconciling classic vertebrate fossil localities with modern biostratigraphy. *Vert. Palaeoasiat.* **49**, 285–310 (2011).
25. Wang, S. Q. et al. Biostratigraphic subdividing of the neogene Dingjiaogou mammalian fauna, Tongxin county, Ningxia province, and its background for the uplift of the Tibetan plateau. *Quat. Sci.* **36**, 789–809 (2016).
26. Qiu, Z. D., Wang, X. M. & Li, Q. Neogene faunal succession and biochronology of central Nei Mongol (Inner Mongolia). In *Neogene Terrestrial Mammalian Biostratigraphy and Chronology of Asia* (eds Wang, X. M., Flynn, L. J. & Fortelius, M.) 155–186 (Columbia Univ., (2013).
27. Zhang, Z. Q. et al. Mammalian biochronology of the late miocene Bahe formation. In *Fossil Mammals of Asia: Neogene Biostratigraphy and Chronology of Asia* (eds Wang, X. M., Flynn, L. J., Fortelius, M. et al.) 187–202 (Columbia University, 2013).
28. Zhu, Y. et al. A new magnetostratigraphic framework for late neogene hipparion red clay in the Eastern loess plateau of China. *Palaeogeogr. Palaeoclimatol. Palaeoecol.* **268**, 47–57 (2008).
29. Peigné, S., Sen, S., Mammifères & de Sansan *Mém. Mus. Natl. Hist. Nat.* (Muséum National d'Histoire Naturelle, Paris, 2012).
30. Drewicz, A. E. Stable Isotope Geochemistry of Bioapatite. Dissertation Boise State University, (2018).
31. Nguy, W. H. & Secord, R. Middle miocene paleoenvironmental reconstruction in the central great plains, USA, from stable carbon isotopes in ungulates. *Palaeogeogr. Palaeoclimatol. Palaeoecol.* **594**, 110929 (2022).
32. Wang, Y. & Deng, T. A 25 m.y. Isotopic record of paleodiet and environmental change from fossil mammals and paleosols from the NE margin of the Tibetan plateau. *Earth Planet. Sci. Lett.* **236**, 322–338 (2005).
33. Zhang, C. F. et al. C4 expansion in the central inner Mongolia during the latest miocene and early pliocene. *Earth Planet. Sci. Lett.* **287**, 311–319 (2009).
34. Zhang, C. F. et al. Diets and environments of late cenozoic mammals in the Qaidam basin, Tibetan plateau: evidence from stable isotopes. *Earth Planet. Sci. Lett.* **333–334**, 70–82 (2012).
35. Passey, B. H., Ayliffe, L. K. & Kaakinen, A. Strengthened East Asian summer monsoons during a period of high-latitude warmth? Isotopic evidence from Mio-Pliocene fossil mammals and soil carbonates from Northern China. *Earth Planet. Sci. Lett.* **277**, 443–452 (2009).
36. Sun, F. J. et al. Paleoecology of pleistocene mammals and paleoclimatic change in South china: evidence from stable carbon and oxygen isotopes. *Palaeogeogr. Palaeoclimatol. Palaeoecol.* **524**, 1–12 (2019).
37. Wang, Y., Cerling, T. E. & MacFadden, B. Fossil horses and carbon isotopes: new evidence for cenozoic dietary, habitat, and ecosystem changes in North America. *Palaeogeogr. Palaeoclimatol. Palaeoecol.* **107**, 269–279 (1994).
38. Passey, B. H. et al. Carbon isotope fractionation between diet, breath CO<sub>2</sub>, and bioapatite in different mammals. *J. Archaeol. Sci.* **32**, 1459–1470 (2005).
39. Tejada-Lara, J. V. et al. Body mass predicts isotope enrichment in herbivorous mammals. *Proc. R. Soc. B.* **285**, 20181020 (2018).
40. Tipple, B. J., Meyers, S. R. & Pagani, M. Carbon isotope ratio of cenozoic CO<sub>2</sub>: a comparative evaluation of available geochemical proxies. *Paleoceanography* **25**, PA3206. <https://doi.org/10.1029/2009PA001851> (2010).
41. Secord, R., Wing, S. L. & Chew, A. Stable isotopes in early eocene mammals as indicators of forest canopy structure and resource partitioning. *Paleobiology* **34**, 282–300 (2008).
42. Shemesh, A. Crystallinity and diagenesis of sedimentary apatites. *Geochim. Cosmochim. Acta.* **54**, 2433–2438 (1990).
43. Sponheimer, M. & Lee-Thorp, J. A. Alteration of enamel carbonate environments during fossilization. *J. Archaeol. Sci.* **26**, 143–150 (1999).
44. Liu, L., Eronen, J. & Fortelius, M. Significant mid-latitude aridity in the middle miocene of East Asia. *Palaeogeogr. Palaeoclimatol. Palaeoecol.* **279**, 201–206 (2009).
45. Janis, C. M. Correlation of cranial and dental variables with body size in ungulates and macropodids. In *Body Size in Mammalian Paleobiology: Estimation and Biological Implications* (eds Damuth, J. & MacFadden, B. J.) 255–299 Cambridge University Press, Cambridge, (1990).
46. Legendre, S. Les communautés de mammifères du paléogène (Eocène supérieur et Oligocène) d'Europe occidentale: structures, milieux et évolution. *Münch. Geowiss. Abh. (A)*. **16**, 1–110 (1989).
47. Costeur, L., Guérin, C. & Maridet, O. Paléoécologie et paléoenvironnement du site miocène de Sansan. *Mém. Mus. Natl. Hist. Nat.* **203**, 661–693 (2012).
48. Legendre, S. Analysis of mammalian communities from the late eocene and oligocene of Southern France. *Palaeovertebrata* **16**, 191–212 (1986).
49. Li, J. et al. Paleo-environment from isotopes and hydrochemistry of groundwater in East Junggar basin, Northwest China. *J. Hydrol.* **529**, 650–661 (2015).
50. Bryant, D. & Froelich, P. A model of oxygen isotope fractionation in body water of large mammals. *Geochim. Cosmochim. Acta.* **59**, 4523–4537 (1995).
51. Wang, Y. et al. Stable isotopes in fossil mammals, fish and shells from Kunlun pass basin, Tibetan plateau: paleo-climatic and paleo-elevation implications. *Earth Planet. Sci. Lett.* **270**, 73–85 (2008).
52. Kaya, F. et al. The rise and fall of the old world Savannah fauna and the origins of the African Savannah biome. *Nat. Ecol. Evol.* **2**, 241–246 (2018).
53. Sun, J. M. et al. Late Oligocene–Miocene mid-latitude aridification and wind patterns in the Asian interior. *Geology* **38**, 515–518 (2010).
54. Miao, Y. et al. What controlled Mid–Late miocene long-term aridification in central Asia? — global cooling or Tibetan plateau uplift: a review. *Earth Sci. Rev.* **112**, 155–172 (2012).

55. Wu, J. B. et al. New magnetic constraints on early-middle miocene uplift of the Liupan shan, Northeastern margin of the Tibetan plateau. *Geochem. Geophys. Geosyst.* **20** <https://doi.org/10.1029/2018GC007944> (2019).
56. Ramstein, G., Fluteau, F., Besse, J. & Joussaume, S. Effect of orogeny, plate motion and land-sea distribution on Eurasian climate change over the past 30 million years. *Nature* **386**, 788–795 (1997).
57. Tang, Z. et al. Late cenozoic central Asian drying inferred from a palynological record from the Northern Tian Shan. *Earth Planet. Sci. Lett.* **302**, 439–447 (2011).
58. Westerhold, T. et al. An astronomically dated record of earth's climate and its predictability over the last 66 million years. *Science* **369**, 1383–1387 (2020).
59. Göhlich, U. B. Order proboscidae. In *The Miocene Land Mammals of Europe* (ed. Rössner, G. E.) 157–168 (Verlag Dr. Friedrich Pfeil, 1999).
60. Sun, D. H. et al. A new elasmothere genus and species from the middle miocene of tongxin, ningxia, china, and its phylogenetic relationship. *J. Syst. Palaeontol.* **21**, 2236619 (2023).
61. Heissig, K. Order Rhinocerotidae. In *The Miocene Land Mammals of Europe* (eds Rössner, G. E. & Heissig, K.) 175–188 (Verlag Dr. Friedrich Pfeil, 1999).
62. Ward, C. T., Crowley, B. E. & Secord, R. Home on the range: a multi-isotope investigation of ungulate resource partitioning at ashfall fossil beds, nebraska, USA. *Palaeogeogr Palaeoclimatol Palaeoecol.* **650**, 112375 (2024).
63. MacFadden, B. J. Equidae. In *Evolution of Tertiary Mammals of North America. Volume 1: Terrestrial Carnivores, Ungulates, and Ungulate-like Mammals* (eds Janis, C. M. et al.) 537–559 (Cambridge University Press, 1998).
64. Sun, B. Y. & Deng, T. New specimens of anchitheriine from the Linxia basin, Gansu and evolution of East Asian anchitheriines. *Chin. Sci. Bull.* **66**, 1479–1489 (2021).
65. O'Connor, D. A., Butt, B. & Fofopoulou, J. B. Foraging ecologies of giraffe (*Giraffa camelopardalis reticulata*) and camels (*Camelus dromedarius*) in Northern kenya: effects of habitat structure and possibilities for competition? *Afr. J. Ecol.* **53**, 183–193 (2015).
66. Janis, C. M. & Manning, E. Antilocapridae. In *Evolution of Tertiary Mammals of North America. Volume 1: Terrestrial Carnivores, Ungulates, and Ungulate-like Mammals* (eds Janis, C. M. et al.) 491–510 (Cambridge University Press, 1998).
67. Webb, S. D. Hornless ruminants. In *Evolution of Tertiary Mammals of North America. Volume 1: Terrestrial Carnivores, Ungulates, and Ungulate-like Mammals* (eds Janis, C. M. et al.) 463–475 (Cambridge University Press, 1998).
68. Habinger, S. G. et al. Isotopic niche modelling of the Pondaung mammal fauna (middle eocene, Myanmar) shows microhabitat differences. Insights into paleoecology and early anthropoid primate habitats. *Front. Ecol. Evol.* **11**, 1110331 (2023).

## Acknowledgements

We thank Burt Wolff and Fajun Sun from Florida State University for their technical assistance in the laboratory; Jie Ye from IVPP for his great guidance on stratigraphy. This work was supported by the National Key Research and Development Program of China (2023YFF0804501); the field work of the Second Tibetan Plateau Scientific Expedition; National Natural Science Foundation of China (42402025; 42472004; 42430207); China Postdoctoral Science Foundation (2024M753179). Stable isotope analyses were performed in the Stable Isotope Lab within Geochemistry Program at the National High Magnetic Field Laboratory supported by US National Science Foundation Cooperative Agreement No. DMR-1644779 and the State of Florida.

## Author contributions

C. L. Writing—original draft, Writing—review & editing, Investigation, Funding Acquisition; S. W. Conceptualization, Writing—original draft, Writing—review & editing, Investigation, Supervision, Funding Acquisition; Y. W. Resources, Writing—review & editing, Funding Acquisition; T. D. Writing—review & editing, Funding Acquisition; J. M., B. W., Q. J., and D. S. Writing—review & editing.

## Competing interests

The authors declare no competing interests.

## Additional information

**Supplementary Information** The online version contains supplementary material available at <https://doi.org/10.1038/s41598-025-10718-3>.

**Correspondence** and requests for materials should be addressed to S.-Q.W.

**Reprints and permissions information** is available at [www.nature.com/reprints](http://www.nature.com/reprints).

**Publisher's note** Springer Nature remains neutral with regard to jurisdictional claims in published maps and institutional affiliations.

**Open Access** This article is licensed under a Creative Commons Attribution-NonCommercial-NoDerivatives 4.0 International License, which permits any non-commercial use, sharing, distribution and reproduction in any medium or format, as long as you give appropriate credit to the original author(s) and the source, provide a link to the Creative Commons licence, and indicate if you modified the licensed material. You do not have permission under this licence to share adapted material derived from this article or parts of it. The images or other third party material in this article are included in the article's Creative Commons licence, unless indicated otherwise in a credit line to the material. If material is not included in the article's Creative Commons licence and your intended use is not permitted by statutory regulation or exceeds the permitted use, you will need to obtain permission directly from the copyright holder. To view a copy of this licence, visit <http://creativecommons.org/licenses/by-nc-nd/4.0/>.

© The Author(s) 2025